Journal of Theoretical Biology 368 (2015) 55–66

Contents lists available at ScienceDirect

Journal of Theoretical Biology

journal homepage: www.elsevier.com/locate/yjtbi

Integrating models to investigate critical phenological overlaps in complex ecological interactions: The mountain pine beetle-fungus symbiosis

Audrey Addison [a,*], James A. Powell [a,1], Barbara J. Bentz [b,2], Diana L. Six [c,3]

[a] Department of Mathematics and Statistics, Utah State University, Logan, UT 84322-3900, USA
[b] USDA Forest Service, Rocky Mountain Research Station, Logan, UT 84321, USA
[c] Department of Ecosystem and Conservation Sciences, The University of Montana, Missoula, MT 59812, USA

HIGHLIGHTS

- Adapt, parameterize and validate model for growth of MPB assoc. fungi within tree.
- Test 5 submodels describing spectrum of possible mycangial packing behavior by MPB.
- Best models describe late mycangial packing; means last fungus is most important.
- Fungal growth scales differently from agar to tree; gives one species an advantage.
- Validates prior knowledge re. fungal differences; may guide future MPB studies.

ARTICLE INFO

Article history:
Received 28 March 2014
Received in revised form
11 December 2014
Accepted 23 December 2014
Available online 31 December 2014

Keywords:
Phenology
Dendroctonus ponderosae
Grosmannia clavigera
Ophiostoma montium

ABSTRACT

The fates of individual species are often tied to synchronization of phenology, however, few methods have been developed for integrating phenological models involving linked species. In this paper, we focus on mountain pine beetle (MPB, *Dendroctonus ponderosae*) and its two obligate mutualistic fungi, *Grosmannia clavigera* and *Ophiostoma montium*. Growth rates of all three partners are driven by temperature, and their idiosyncratic responses affect interactions at important life stage junctures. One critical phase for MPB-fungus symbiosis occurs just before dispersal of teneral (new) adult beetles, when fungi are acquired and transported in specialized structures (mycangia). Before dispersal, fungi must capture sufficient spatial resources within the tree to ensure contact with teneral adults and get packed into mycangia. Mycangial packing occurs at an unknown time during teneral feeding. We adapt thermal models predicting fungal growth and beetle development to predict overlap between the competing fungi and MPB teneral adult feeding windows and emergence. We consider a spectrum of mycangial packing strategies and describe them in terms of explicit functions with unknown parameters. Rates of growth are fixed by laboratory data, the unknown parameters describing various packing strategies, as well as the degree to which mycangial growth is slowed in woody tissues as compared to agar, are determined by maximum likelihood and two years of field observations. At the field location used, the most likely fungus acquisition strategy for MPB was packing mycangia just prior to emergence. Estimated model parameters suggested large differences in the relative growth rates of the two fungi in trees at the study site, with the most likely model estimating that *G. clavigera* grew approximately twenty-five times faster than *O. montium* under the bark, which is completely unexpected in comparison with observed fungal growth on agar.

© 2014 Elsevier Ltd. All rights reserved.

1. Introduction

Most organisms are involved in multiple symbioses, and for many, at least some of these partnerships are obligate and necessary for survival. However, the phenologies of interacting partners are often differentially influenced by environmental conditions and this can affect their ability to interact at critical junctures in their life histories.

* Corresponding author. Tel.: +1 435 797 1953.
E-mail addresses: audrey.smith@aggiemail.usu.edu (A. Addison), jim.powell@usu.edu (J.A. Powell), bbentz@fs.fed.us (B.J. Bentz), diana.six@cfc.umt.edu (D.L. Six).
[1] Tel.: +1 435 797 1953.
[2] Tel.: +1 435 755 3577.
[3] Tel.: +1 406 243 5573.

http://dx.doi.org/10.1016/j.jtbi.2014.12.011
0022-5193/© 2014 Elsevier Ltd. All rights reserved.

The issue of phenological overlap in ecology is not new; it has long been known that many species interact in ways that require fairly precise alignments of particular life stages of the interactants. For example, phenological synchronicity between pollinators and flower production is critical for the reproduction of many plants (Gross and Werner, 1983; Murali and Sukumar, 1994). In some insect species, different development rates or maturation times for males and females can result in the loss of reproductive success under some conditions (Kaspari et al., 2001), and can increase the risk of extinction in small populations (Calabrese and Fagan, 2004). For pathogens and parasites, infection often depends on phenological overlap between the pathogen or parasite and susceptible individuals (Molnár et al., 2013). Because phenological overlaps are critical for many biological interactions, being able to connect phenological models for multiple, interacting species would greatly increase our understanding of how environmental conditions influence complex ecological interactions and their outcomes. However, modeling approaches which account for phenological overlap and interaction have not been developed.

In this paper, we connect models for a multipartite symbiosis that exists among a beetle and two mutualistic fungi to investigate a key phenological overlap that must occur for the symbiosis to persist, an overlap with substantial fitness effects on all three partners depending upon outcomes. Our system consists of mountain pine beetle (MPB, *Dendroctonus ponderosae*, Coleoptera: Curculionidae, Scolytinae) and two mutualistic fungi, *G. clavigera* and *O. montium*. This system is highly appropriate for developing an integrated modeling approach. It involves multiple interacting species, each with different temperature tolerances that must synchronize specific phases of their life histories at a particular point in time to persist. All three organisms are ectotherms and our results will be broadly applicable to other ectothermic systems which include the majority of symbiotic systems on Earth. In addition, the MPB is currently the most significant insect species affecting pines in western North America. Between 1997 and 2010, MPB caused tree mortality on more than 8.5 million forested ha in British Columbia and the western United States combined (Meddens et al., 2012) and range expansions in Alberta and northern British Columbia are ongoing (de la Giroday et al., 2012) as a result of warming summers and winters (Cudmore et al., 2010; Sambaraju et al., 2012). The interdependence of the partners in this symbiosis make it is essential to incorporate the dynamics of all three species when modeling or attempting to predict future MPB-caused tree mortality or estimating range expansions or contractions.

1.1. The MPB-fungus system

MPB has evolved a complex mutualism with two species of filamentous fungi, *G. clavigera* and *O. montium* (Adams et al., 2008; Six, 2012). Following successful attack and colonization of a host tree, adult MPB excavate tunnels under the bark and lay eggs. During this process, they simultaneously inoculate phloem tissue with fungal spores from specialized fungal transport structures called mycangia (Six and Paine, 1998). After this, the beetles and fungi develop at rates based on temperature. During development, the larvae feed on both phloem and fungal hyphae. The fungi concentrate nitrogen in the tissues upon which the larvae feed, supporting greater beetle size and survival (Bleiker and Six, 2007). Prior to emergence, the newly enclosed (teneral) adults feed on fungal spores (Six and Paine, 1998). Spore feeding is essential to adult beetle reproduction (Six and Paine, 1998). The teneral feeding period is variable in length, ranging from a few days to weeks depending upon temperature. Sometime during this period of spore feeding, the mycangia become packed with fungal spores which are then dispersed to the next host tree and the next generation of beetles. The proportion of each fungal species dispersed by each generation is determined by the timing and extent of fungal growth within the tree and acquisition of spores in mycangia by teneral adult MPB.

Whether a fungus is acquired in the mycangia of a beetle, as well as which fungus is acquired, is an important aspect of this mutualism. The beetle needs at least one fungus to survive. However, the fungi are not equivalent in value to the insect (Bleiker and Six, 2007). *G. clavigera* concentrates nitrogen better than *O. montium* (Cook et al., 2010) which may account for observations that beetles developing with *G. clavigera* are bigger and have higher productivity and survival rates than those developing with *O. montium* (Six and Paine, 1998; Bleiker and Six, 2007). Because of the dissimilar fitness effects on the beetle, differences in the relative prevalence of the two fungi in a population are likely to strongly influence beetle population dynamics.

The relative prevalence of the two fungi is primarily determined by temperature which differentially affects fungal growth, sporulation, and competition. The two fungi grow at different rates in response to temperature (Six and Paine, 1998; Moore., 2013). This difference is substantial enough to allow for temporal niche separation (Moore., 2013), albeit incomplete, and to avoid competitive exclusion by one or the other fungus under at least some conditions (Addison et al., 2013). Temperature also influences the outcome of competition between the two fungi. The two fungi exhibit exploitation competition where the outcome is determined by the rate of resource capture. They do not exhibit antagonism and do not capture resource that has already been captured by a conspecific or heterospecific competitor (Bleiker and Six, 2009; Moore., 2013). Therefore the outcome (area within a tree that is captured by each fungus and available to teneral hosts for dispersal) directly depends on the temperature-dependent rate of growth of each fungus within the tree. Furthermore, because these two symbionts differ substantially in their effects on beetle fitness, their relative prevalence with dispersing beetles is doubly important, affecting both fungal fitness as well as the fitness of subsequent beetle populations. We also note that temperature affects sporulation, however, both fungi sporulate at the temperature range that supports eclosion of teneral MPB (Moore., 2013) so this is not further analyzed in this paper.

To connect phenological models for the MPB-fungus system, several components need to be considered. These include (1) the presence of not one but two differentially responding mutualistic fungal species, (2) the fact that phenological outputs are qualitatively different (developmental milestones for MPB versus spatial extent for fungi), and (3) the range of biologically plausible ways in which MPB procure fungal spores during the teneral feeding window. Because the two fungi compete for the same spatial resources under bark, their relative rates of growth and resource capture must be included in models. Phenological models for MPB provide temporal predictions of MPB life stage timing (Bentz et al., 1991; Logan and Bentz, 1999; Régnière et al., 2012). The completion of fungal life stage events, however, is not relevant in this context as the fungi only sporulate in beetle pupal chambers and all other growth is by somatic hyphae. Therefore, models for the growth of these fungi are based on, and predict measurements of, length of phloem colonized (Addison et al., 2013). These different outputs from beetle and fungal models need to be combined in a tractable way. Finally, interactions between MPB and their fungal symbionts take place exclusively within the phloem layer of a tree. Although some types of interactions have been measured within this cryptic habitat (Adams and Six, 2007; Bleiker and Six, 2007), others, such as how and when MPB pack their mycangia with fungi and how fungal growth rates determined from lab studies in artificial media, scale to actual growth rates in a tree, are completely unstudied.

1.2. MPB-fungus interaction and mycangial packing

Timing of MPB mycangial packing influences which fungus is transported from a brood tree to a new tree. MPB feed on fungal spores as teneral adults (Adams and Six, 2007), packing their mycangia with spores sometime following eclosion from the pupa but prior to emerging from the host tree (Six and Paine, 1998). The feeding window between pupal eclosion and emergence varies from days to weeks. During this time fungal prevalence, and thus the potential for a fungus to be acquired and dispersed by MPB, may change drastically. Timing and efficiency of mycangial packing is thus critical for predicting future fungal prevalence. To better predict fungal acquisition by teneral adults, we hypothesize and test five possible strategies for the timing of mycangial packing. These strategies describe a spectrum of behaviors ranging from model 1, in which MPB immediately pack their mycangia with the first fungus available, to model 5, in which they delay mycangial packing until just prior to emerging from the tree.

Our goals were to use field observations to quantify under-bark growth rates of the two fungal species and evaluate MPB mycangial packing hypotheses. We construct likelihood functions connecting mathematical hypotheses with field observations of fungi carried by emerging MPB adults, with unknown parameters representing five mycangial packing hypotheses and scaling fungal growth rates. Using the field observations, we explore which mycangial packing strategy would be most likely and evaluate the final model. Finally, we discuss our findings in relation to the MPB-fungus system and suggest follow-up studies that would further our understanding of mechanisms involved in mycangial packing, and ultimately, fungal prevalence the following year and with the next generation of beetles. While our approach is specific to the MPB-fungus system, elements of our approach (representing differential thermal responses, allowing for a spectrum of interactions during a period of cryptic phenological overlap, parsing the combined models in terms of likelihood and model competition) can be adapted to connect phenological models in other systems with interacting, ectothermic species.

2. Methods

2.1. MPB, fungi and temperature data collection

The timing of MPB attacks on trees and adult emergence the following summer was monitored on three lodgepole pine (*Pinus contorta*) in 2010–2011 and four lodgepole pine in 2011–2012 at a site in Logan Canyon, UT (41.9528, −111.55290, 2190 m). The MPB population in the vicinity of the site was in the vacinity considered an incipient epidemic. In addition to monitoring timing of attack and emergence of adult MPB, identity of fungal associates (i.e., *G. clavigera* and *O. montium*) carried by MPB entering and exiting trees was determined through phloem sampling and mycangial dissection of adults.

2.1.1. MPB attack timing

On 2 August 2010, an aggregation lure (Synergy Semiochemicals Corporation, Burnaby, BC, Canada) was placed on the north side of each tree. After 10–15 MPB attacks were observed on a tree (1–3 days) the lure was removed to allow the MPB attack process to continue naturally. Attacks were monitored daily on each tree between one and five feet above the ground by bole quadrant (i.e., north, south, east and west). MPB attacks are visible as frass or resin exuding from small entrance holes through the bark. Each day's attacks were marked with a different colored straight pin, summed and recorded. This process was repeated in 2011 in the same vicinity using new live trees.

2.1.2. Fungal samples from attacking MPB

Our protocol assumed that fungi introduced into a tree by individual MPB will be present in the phloem directly surrounding its entry site soon after beetle entry. The fungi are inoculated by MPB and grow very slowly at the beginning of the colonization period. Thus any fungi found growing at a beetle entry point can be assumed to have come from the beetles that initiated that attack/gallery. To allow adequate time for the fungi to grow into the phloem following adult MPB attacks, we waited 10 days after the first attacks to begin sampling trees. On the 10th day following the first day of attack, 12 attack sites were randomly chosen from all attacks that occurred on a single tree over the first three days. These areas were prepared for fungal sampling by smoothing the bark just above the entry hole (MPB tunnel upward after entry) and spraying the area with 70% ETOH. Using a ETOH sterilized 9 mm cork borer, a core containing bark and phloem was removed from just above the entry hole. The phloem portion was placed into a sterile-autoclaved microcentrifuge tube labeled with tree number, date of MPB attack, and sampling date, then placed on ice and transported to the laboratory. This process was repeated for each tree every day throughout the attack period, resulting in up to 120 samples per tree.

To identify the fungal species present, each phloem sample was placed in the center of a Petri dish containing 2% malt extract agar amended with Streptomycin and cycloheximide and stored at room temperature for 1 week to allow fungal growth. Isolates were then identified using cultural characteristics and morphology of conidia and conidiophores.

2.1.3. MPB emergence timing

In both years following successful attack, mesh cages were placed on all four quadrants of each tree covering the entire sample area. Emerging univoltine beetles were collected from cages daily. Beetles were transported to the laboratory and placed in sterile Petri dishes with filter paper moistened with distilled water and stored at 3 °C for less than one week. Each adult beetle's sex was determined and the width of its pronotum was measured. Both mycangia of each live beetle were dissected and placed individually on opposite sides of a Petri dish containing 2% malt extract agar amended with Streptomycin and cycloheximide. Each dish was labeled with a unique code that identified a single beetle so that fungal identification could be cross-referenced to the tree, bole quadrant, emergence date, size and sex. A maximum of 20 adult MPB from each of the four quadrants of each sampled tree were dissected per sample day (i.e., 80 beetles per day). Fungal cultures were grown at room temperature (~21 °C) and then identified to species.

Length of the MPB life cycle in trees attacked in 2010 was predominately univoltine (i.e., one generation in a single year), although ~20% of the population was semivoltine (i.e., one generation every two years) (Bentz et al., 2013). MPB in trees attacked in 2011 were 100% univoltine. Only data from univoltine beetles from 2010 attacks were used in model parameterization, and data from trees attacked in 2011 were used in model validation.

2.1.4. Temperature measurements

Ambient air temperature was measured at the study site using a radiation-shielded temperature probe placed at 1.4 m above the ground on the north side of a tree to reduce direct sun exposure (Campbell Scientific Inc., Logan UT). North and south bole aspect phloem temperatures were measured using thin-tipped (0.34 mm^2) thermocouple temperature probes (Omega Engineering, Inc., Stamford, DT) inserted under the bark and into the phloem layer. Hourly air and phloem temperatures were collected

continuously over both sampling years (May 27, 2010 through November 8, 2012) using a datalogger (Campbell Scientific Inc., Logan UT). Model performance was tested using each of the temperature records to explore the effect of north versus south bole temperatures and to determine how the model might perform for a different site if only ambient temperatures are available.

2.2. Fungal growth model

G. clavigera and *O. montium* spread outward in an infested tree by forming a mycelial network from their initial inoculation point. Because the fungi grow under bark, it is impossible to monitor growth from individual inoculation points in a tree over time. Instead, growth rates were determined in lab experiments by growing the two fungi on 2% malt extract agar in Petri dishes at six temperatures (Moore., 2013). These data were used to develop the fungal growth rate curves and growth rate parameters discussed in Addison et al. (2013). The dependence of the rate curve for each species on temperature is assumed to follow

$$r(T) = \begin{cases} B(e^{\alpha(T-T_0)}-1) - B(e^{\alpha(T_m-T_0)}-1)e^{(T-T_m)/b}, & T \in (T_0, T_m) \\ 0, & T \neq (T_0, T_m), \end{cases} \tag{1}$$

which is a modal response curve with upper, T_m, and lower , T_0, thresholds and a strong optimum which is a short distance, b, below the optimum. This generic curve has been used to model thermal responses of arthropods (Logan et al., 1976), trees (Lehning et al., 2001), fish (Salinger and Anderson, 2006) and fungi (Köhl et al., 1999). The parameters α and B control shape and magnitude of the response. Parameters for each fungal species were estimated using maximum likelihood estimation (MLE) techniques to best match hundreds of fungal growth observations for each species (Addison et al., 2013) (see Fig. 1). Specific parameter values used for the two fungi are given in Table 1.

2.2.1. Fungal colonization index in a tree

Total distance colonized by a fungus from an initial point of attack can, in principle, be predicted using direct integration of the growth curves. However, a concern with using laboratory growth rates directly is that conditions inside the tree are different than those in artificial media on a Petri dish. Within trees, fungi encounter tree defensive chemicals and moisture levels that can act to slow their growth rates relative to those that occur in the lab. The result of inoculation studies of these fungi in trees also suggest that *G. clavigera* is a better first invader of a tree (Krokene and Solheim, 1998) than *O. montium* because it is more tolerant of tree defenses and low oxygen contents in recently colonized phloem. To account for this in our model, we incorporate growth rate scaling parameters, β, for each species, and calculate the total distance colonized from a point of inoculation on day t_a (of, for example, *G. clavigera*),

$$\text{Distance } Gc \text{ colonized starting } t_a = \beta_{GC} \int_{t_a}^{t} r[T(\tau)]\, d\tau,$$

for a given temperature profile, $T(t)$. The cumulative length colonized by *G. clavigera* in the entire tree is then given

$$Cum_{GC}(t) = \sum_{t_a < t} (\text{Fraction } Gc \text{ starting day } t_a) \times (\text{Distance } Gc \text{ colonized starting } t_a).$$

The units of $Cum_{GC}(t)$ are length; to create a colonization index (or approximate fraction of available area colonized) we normalize by the expected distance between MPB attacks, C. Considering only MPB attack densities high enough to cause tree mortality, the average space between fungal inoculations, C, can range from

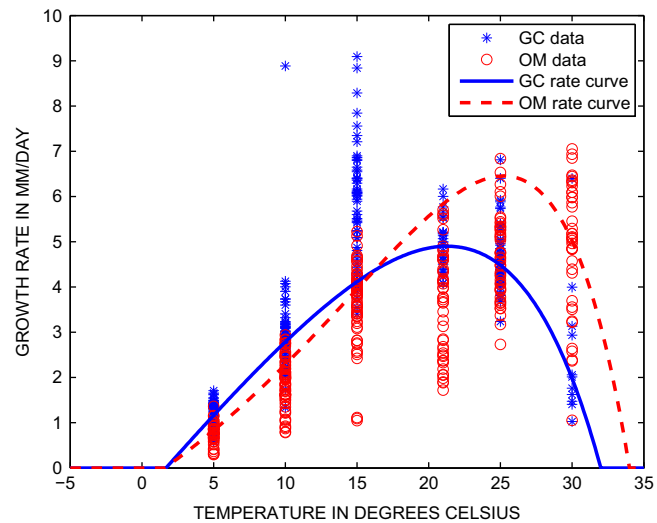

Fig. 1. Growth rate observations in culture for *G. clavigera*, GC (*), and *O. montium*, OM (o), are shown with their respective growth rate curves (solid line for *G. clavigera* and dashed line for *O. montium*) using Table 1 parameters. *G. clavigera* has a higher rate of growth when temperatures lie below approximately 16 °C and *O. montium* has a higher rate of growth for temperatures above 16 °C, indicating some thermal niche separation.

Table 1
Parameters for the fungal growth rate curves: α affects the rate of increase at low temperatures, b is the thickness of the boundary layer between peak growth and the upper temperature threshold, B is a scaling factor which affects the maximum rate of fungal growth, while T_0 and T_m are the lower and upper temperature thresholds for the fungi respectively in °C. These parameters were estimated in Addison et al. (2013).

Parameter values for fungal growth rate curves					
Fungus type	α	b	B	T_0 (°C)	T_m (°C)
G. clavigera	0.0041	8.0407	95.6120	0.9123	32
O. montium	0.0662	7.4949	3.8395	−0.0236	34

approximately 40 mm to approximately 85 mm (Addison et al., 2013). For simulations in this paper we used $C = 54$ mm corresponding to an optimal MPB attack density of 62 MPB/m^2 (Raffa and Berryman, 1983). Letting p be the earliest day at which the two colonization indices sum to one (so that the tree may not be over-colonized), the index for each species is given by

$$p_{GC}(t_j) = \begin{cases} \beta_{GC} \cdot \frac{Cum_{GC}(t_j)}{C} & \text{for } t_j < p, \\ \beta_{GC} \cdot \frac{Cum_{GC}(p)}{C} & \text{for } t_j \geq p, \end{cases} \tag{2}$$

and

$$p_{OM}(t_j) = \begin{cases} \beta_{OM} \cdot \frac{Cum_{OM}(t_j)}{C} & \text{for } t_j < p, \\ \beta_{OM} \cdot \frac{Cum_{OM}(p)}{C} & \text{for } t_j \geq p, \end{cases} \tag{3}$$

where

$$\beta_{GC}\frac{Cum_{GC}(p)}{C} + \beta_{OM}\frac{Cum_{OM}(p)}{C} = 1.$$

Because dispersal to new host trees depends on the overlapping phenology of the fungal species and MPB, we next need to determine the probability distribution describing the timing of MPB teneral adult feeding (Fig. 2).

2.2.2. Predicting the timing of teneral adult feeding on fungi

To predict what fungus would be observed in a mycangium on a given emergence day, t_k, we need to know the relative likelihood

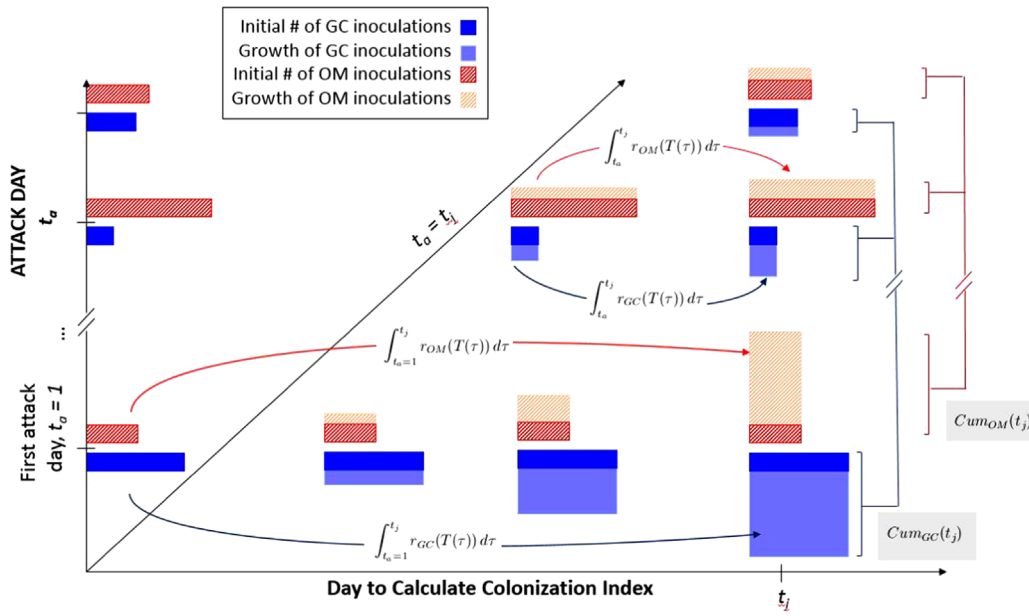

Fig. 2. Inoculations of *G. clavigera* and *O. montium* into a tree will vary daily depending on the number of attacking MPB carrying each fungus each day. In the figure, the number of inoculations is represented by the length of the horizontal bar for each species on a given attack day t_a. Growth of each fungal species is calculated based on the species-specific growth rate (dependent on hourly temperature) scaled by the number of MPB carrying each fungus into the tree on each attack day. This is represented by the widening of the horizontal bars. It is calculated for each day of attack and the cumulative growth of each fungal species is obtained by summing the growth of inoculations carried into the tree prior to the day of interest, day t_j. Following the last attack, cumulative growth of each fungal species is no longer influenced by the number of new inoculations.

of the teneral adult feeding upon spores on an earlier day, t_j. The probable feeding window distribution can be determined by working backward from a distributional MPB phenology model (Régnière et al., 2012) using observed hourly temperatures and known attack and emergence dates. The probability that the teneral stage lasts from t_j to t_k can be expressed $t_k - t_j = \delta \cdot \tau$ where τ is the median development time for MPB adults, and δ is a random variable with mean one. Solving for δ we find that

$$\delta = \frac{t_k - t_j}{\tau} = \int_{t_j}^{t_k} r_{\mathrm{MPB}}[T(t')]\,dt', \tag{4}$$

where r_{MPB} represents the teneral adult development rate of MPB as a function of temperature T. We use the functional form and parameters for teneral adult development given in (Régnière et al., 2012) and follow those authors in assuming δ is lognormal, i.e. $\delta = e^{\epsilon}, \epsilon \sim \mathrm{N}\left(-\frac{1}{2}\sigma^2, \sigma^2\right)$. The cumulative distribution function of development time is

$$P(t > t_j) = \Phi\left[\frac{\ln(\delta) + \sigma^2/2}{\sigma}\right],$$

so the probability density function (pdf) of t_j being during the teneral stage can be expressed as

$$\frac{dP}{dt_j} = \frac{1}{\sqrt{2\pi\sigma^2\delta^2}} \exp\left(-\frac{(\ln(\delta) + \sigma^2/2)^2}{2\sigma^2}\right) \cdot \frac{d(\delta)}{dt_j}.$$

Using

$$\frac{d(\delta)}{dt_j} = -r(T(t_j)),$$

the probability that a beetle emerging at time t_k was feeding as a teneral adult at time t_j is given by

$$pdf_k(t_j) = \frac{r(T(t_j))}{\sqrt{2\pi\sigma^2 R(t_j, t_k)^2}} \exp\left(-\frac{(\ln(R(t_j, t_k)) + \sigma^2/2)^2}{2\sigma^2}\right). \tag{5}$$

Here

$$R(t_j, t_k) = \int_{t_j}^{t_k} r(T(t'))\,dt'.$$

Numerical integration was performed with hourly time steps and the trapezoid rule summed on a daily basis. The continuous function pdf_k is approximated by a daily probability of feeding on day t_j given emergence on day t_k,

$$P_{\mathrm{feed}}(t_j, t_k) = pdf_k(t_j). \tag{6}$$

An example of the resulting distribution of teneral adult feeding can be seen in Fig. 3 where the distribution of possible feeding start days is shown for a particular day of emergence. Note that this calculation reflects the probability that an adult could emerge on day t_k, given that it happens to be under the bark on day t_j. It does not reflect the actual probability of teneral adults appearing on day t_j under the bark given observed attacks. The calculation therefore may assign a nonzero probability to teneral adult feeding at times when teneral adults would not be present based on the MPB phenology model. When nonzero probabilities of teneral adult feeding occurred at times when teneral adults were not actually present we set the probabilities to zero.

2.2.3. Probabilistic models for mycangial packing

Using the feeding probabilities, P_{feed}, and the proportion of each fungus available in the tree (p_{GC} and p_{OM}) over time, we can construct submodels to compare five mycangial packing hypotheses. The strategies describe a spectrum of behaviors ranging from model 1, in which MPB immediately pack their mycangia with the first fungus available, to model 5, in which they delay mycangial packing until just prior to emerging from the tree. In the following discussion, p_1, p_2 and p_3 will represent the proportion of MPB emerging on day t_k with *G. clavigera*, *O. montium*, and no fungus respectively. How

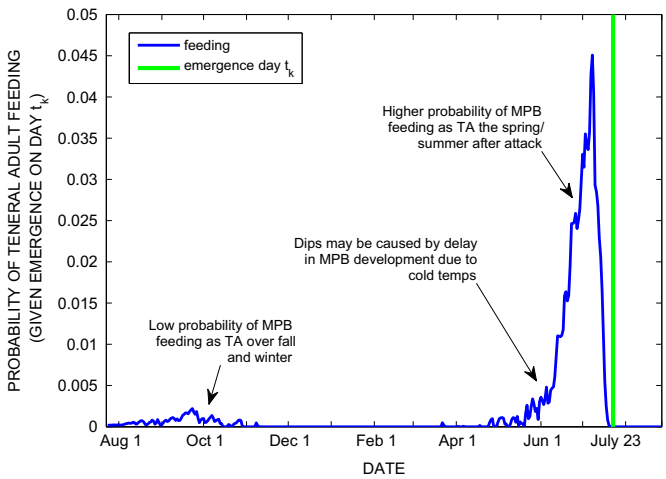

Fig. 3. Predicted probability of feeding as a teneral adult given emergence on July 23. The emergence day is shown as a vertical line. The most likely time for a MPB to be feeding on fungal spores is in the weeks leading up to emergence from a tree (though there is some nonzero, but very low, probability – based on the phenology model – that this could occur in late fall or early spring). The dips in the curve are cold-induced delays in progress from the pupal to teneral adult stage.

p_1, p_2 and p_3 are calculated depends on mycangial packing hypothesis:

(1) *First fungus contacted* – the fungus present in mycangia is the first fungus contacted by the beetle. For each emergence day t_k, probability of acquiring a fungal spore on day t_j is the product of the colonization index and the probability of t_j being within the feeding window. Summed over all possible feeding days the probabilities p_1, p_2 and p_3 become

$$p_1(t_k) = \sum_{t_j} p_{GC}(t_j) P_{\text{feed}}(t_j, t_k),$$
$$p_2(t_k) = \sum_{t_j} p_{OM}(t_j) P_{\text{feed}}(t_j, t_k), \quad \text{and}$$
$$p_3(t_k) = 1 - p_1(t_k) - p_2(t_k).$$

(2) *Mostly first fungus contacted* – probability of open space remaining in the mycangia is assumed to decrease exponentially, with parameter λ which represents the mean time to fill mycangia. The probability P of first encountering a fungal spore after t days is

$$P(\text{first encounter at } t \text{ days}) = e^{-t/\lambda},$$

so the probability of not encountering a fungus until time t is given by

$$F(t) = P(\text{no encounter} \le t) = 1 - e^{-t/\lambda}.$$

The probability that a mycangia is packed day t_j is

$$p_{pack}(t_k - t_j) = F(t_k - t_j) - F(t_k - t_j - 1). \tag{7}$$

Then

$$p_1(t_k) = \sum_{t_j} p_{GC}(t_j) p_{pack}(t_k - t_j) P_{\text{feed}}(t_j, t_k), \quad \text{and}$$
$$p_2(t_k) = \sum_{t_j} p_{OM}(t_j) p_{pack}(t_k - t_j) P_{\text{feed}}(t_j, t_k).$$

(3) *Delayed mycangial packing* – a Laplace probability distribution allows for an initial delay of μ days in mycangial packing due to a lag in sporulation or mycangial maturity. Space availability in mycangia is assumed to fall exponentially away from this mean. Mathematically, this changes the probability of not encountering a fungus until time t to

$$P(\text{no encounter} \le t) = \begin{cases} \frac{1}{2} e^{(t-\mu)/\lambda} & \text{for } t < \mu \\ 1 - \frac{1}{2} e^{(t-\mu)/\lambda} & \text{for } t \ge \mu, \end{cases} \tag{8}$$

where λ is mean time to pack mycangia. The remaining calculations for p_1, p_2 and p_3 are identical to those for model 2.

(4) *Mostly last fungus contacted* – probability of maintaining residency in mycangia is assumed to decrease exponentially in time (so that the most recently encountered fungi are most likely to be present). Probabilistically,

$$P(\text{no encounter} \ge t) = 1 - e^{-(t_k - t)/\lambda},$$

where t_k is the day of emergence and λ is the mean residence time. Using this CDF calculations for p_1, p_2 and p_3 are identical to those for model 2.

(5) *Last fungus contacted* – fungi present in mycangia are those available immediately prior to emergence. Then

$$p_1(t_k) = p_{GC}(t_k) \quad \text{and} \quad p_2(t_k) = p_{OM}(t_k).$$

Differences among the feeding models are shown in Fig. 4.

2.2.4. Likelihood function for parameterizing the fungus growth model

MPB field observations were divided into categories in which n_1 represented the number carrying *G. clavigera*, n_2 represented the number carrying *O. montium*, n_3 represented the number carrying no fungi, and $N = n_1 + n_2 + n_3$ represented the total number of MPB emerging for each observed emergence day. These numbers, along with p_1, p_2 and p_3 representing proportions of *G. clavigera*, *O. montium*, and no fungi in mycangia on a given emergence day, give a multinomial likelihood for daily observations,

$$\mathcal{L} = \prod_{t_k} \frac{N(t_k)!}{n_1(t_k)!\, n_2(t_k)!\, n_3(t_k)!} p_1(t_k)^{n_1(t_k)} p_2(t_k)^{n_2(t_k)} p_3(t_k)^{n_3(t_k)}. \tag{9}$$

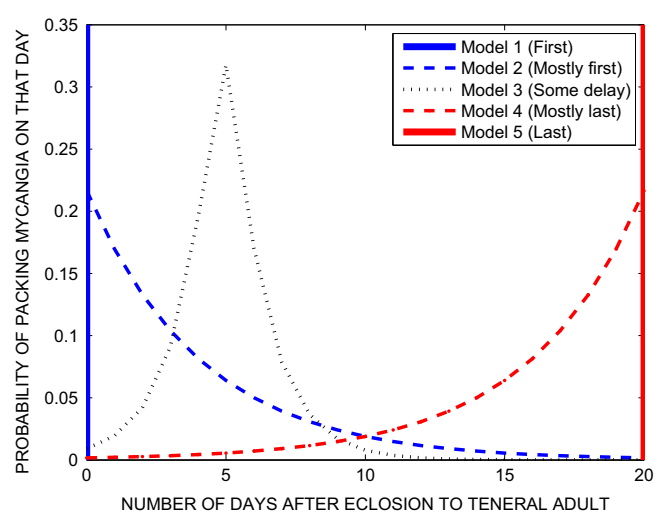

Fig. 4. Comparing distributions in mycangial packing models. In model 1, mycangial packing takes place on day 1 of teneral adult feeding, in model 2, packing begins immediately after eclosion to the teneral adult stage, model 3 allows a delay then a peak in packing, model 4 results in little mycangial packing until just before adult emergence (in this case occurring 20 days after entering the teneral adult life stage), and in model 5 packing takes place the day before emergence. For models 2 and 4 $\lambda = 4.1$; $\lambda = 1.3$ and $\mu = 5.4$ for model 3.

The parameters β_{GC}, β_{OM}, λ and μ are determined to maximize likelihood using a built-in MATLAB optimizer (the Nelder-Mead simplex algorithm, `fminsearch`).

The two parameters with largest potential to impact are β_{GC} and β_{OM}, the growth rate scaling parameters for *G. clavigera* and *O. montium*, respectively. We constrain and assess their values based on several assumptions:

(1) we hypothesize that fungi grow slower in a tree than in a Petri dish and that they will not lose resources once they have been acquired (this requires β_{GC} and β_{OM} to lie between 0 and 1),
(2) based on observations of MPB occasionally tunneling backwards in their larval galleries to eat fungus colonized phloem (Adams and Six, 2007), we obtained a rough estimate for a single growth rate scaling parameter, $\beta = 0.1387$, for both fungi in Addison et al. (2013); and
(3) *G. clavigera* is known to be more aggressive at growing in a freshly killed tree (Krokene and Solheim, 1998) and may be less susceptible to cold induced mortality than *O. montium* (Rice et al., 2008) which leads us to expect that β_{GC} will be larger than β_{OM}.

Practically, constraints were implemented by setting the negative log likelihood to an arbitrarily large positive number when $\beta < 0$ and an arbitrarily large number times β when $\beta > 1$. The optimization procedure was repeated 1000 times for each model with random initial guesses for each parameter. Parameters resulting in the lowest negative log likelihood were selected as the best parameter estimates for each model.

2.3. Bootstrapping the data

To quantify the sensitivity of parameter estimates, we employed bootstrapping, constructing a new set of observations (i.e., MPB emergence date and species of fungus carried, $n_1(t_k)$, $n_2(t_k)$ and $n_3(t_k)$) of the same size as the original dataset by sampling the original dataset with replacement. After obtaining a new set of observations, the model and the MLE procedure was repeated 1000 times to generate a 95% confidence interval for parameters.

2.4. Testing model sensitivity to temperature

Sensitivity of the models to temperature was tested by running models 1–5 using their respective parameter estimates (Table 3) with field-collected ambient temperature, and north and south bole phloem temperatures collected for each tree. We also ran models 1–5 using observed temperatures from trees attacked in 2010, increased and decreased by -1.5 to 1.5 °C (incremented by 0.05 °C). For each of the modified temperature sets, model predictions for all five models were compared against observed MPB emergence and fungal associate.

Table 2
Comparison of the percentages of MPB carrying *G. clavigera* (GC), *O. montium* (OM), both fungi, or no fungi into and out of trees attacked in 2010 and 2011.

Dataset	**Attack and emergence data**				
	# of MPB analyzed	% GC	% OM	% Both	% None
2010 attacks	263	21.8	38.6	4.9	34.7
2010 emergence	1099	90.4	4.3	3.5	1.9
2011 attacks	193	26.9	28.8	1.3	42.9
2011 emergence	908	63.9	10.8	6.2	19.2

2.5. Model evaluation and validation

Output from the five mycangial packing models were compared using Akaike Information Criterion (AIC), defined as

$$\mathrm{AIC} = -2\log(\mathcal{L}) + 2K,$$

where $\mathcal{L}$ is the likelihood of the model (9) and K is the number of parameters (Burnham and Anderson, 2002). This value quantifies the amount of information lost by the model and allows for model competition via AIC. Models were also compared using R^2. Model validation was attempted using an independent data collected from trees attacked in 2011. The model was initiated with observed 2011 attacks and driven by observed temperatures and estimated parameters for 2010 to predict fungal prevalence on emerging MPB. Predicted results were compared to observed prevalence of fungi being carried by emerging MPB.

3. Results

3.1. Parameter estimates for the five mycangial packing models

MPB attack and emergence observations and associated data on the prevalence of fungi on emerging adults from trees attacked in 2010 (Table 2) were used to obtain estimates of the growth rate scaling parameters β_{GC} and β_{OM} and mycangial packing parameters λ and μ (as applicable) for the five mycangial packing models (Table 3). Model parameterization was repeated for ambient air temperatures as well as north and south bole phloem temperatures for the various attacked trees. While there were slight differences in parameter estimates, the models performed equally well regardless of temperature. For consistency, we chose to parameterize the models using north bole phloem temperatures. The results of this parameterization show some variability between β_{GC} and β_{OM} across models (and across acceptable parameters for model 4), however, the ratio of the two parameters β_{GC}/β_{OM} remains quite steady, ranging from just

Table 3
Comparison of the growth rate scaling parameter estimates β_{GC} and β_{OM} and feeding distribution parameters λ (the mean waiting time to encounter fungi; models 2–4), and μ (the peak receptivity to fungal spores; model 3), obtained using maximum likelihood for 2010 data. Parameter estimation for model 4 was slightly less consistent than for models 1–3 and 5, so the midpoint of the acceptable parameters that resulted in the best AIC has been reported. Note that the ratio of the growth rate scaling parameters was largely steady across all models.

Dataset	**Estimated parameters for 2010**				
	Model 1	Model 2	Model 3	Model 4	Model 5
β_{GC}	0.9336	1.0000	1.0000	0.8959	0.6355
β_{OM}	0.0376	0.0401	0.0401	0.0364	0.0263
β_{GC}/β_{OM}	24.81	24.92	24.92	24.62	24.16
λ	Na	3.7054	1.2883	4.1333	Na
μ	Na	Na	5.4168	Na	Na

Table 4
Comparison of $\Delta\mathrm{AIC} = \mathrm{AIC} - \mathrm{AIC}_{low}$ computed for the various mycangial packing hypotheses for 2010 data. Models are arranged from packing early (model 1) to packing late (model 5) and the best ΔAIC values are marked in bold. Model 5 produced the lowest AIC for 2010, $\mathrm{AIC}_{low} = 247.4722$ with model 4 producing a very similar AIC, indicating mycangial packing occurs late in the teneral adult feeding window.

Comparison of ΔAIC (**2010 data**)				
Model 1	Model 2	Model 3	Model 4	Model 5
4.9927	7.1009	6.3786	**2.4208**	**0**

24.16 to 24.92. Comparing the estimates for β_{GC} and β_{OM} shown in Table 3 with assumptions described in Section 2.2.4, all the estimates seem reasonable. Each value for β_{GC} and β_{OM} lies between 0 and 1, the average of the parameters lies reasonably close to our former estimate of $\beta = 0.1387$ (Addison et al., 2013), and the estimates for the *G. clavigera* scaling parameter are much greater than for *O. montium*. This difference between the β_{GC} and β_{OM} estimates reflected the MPB emergence observations (Table 2), which were heavily biased toward *G. clavigera*. MPB that attacked trees in both 2010 and 2011 were observed carrying a nearly equal mix of *G. clavigera* and *O. montium* whereas emerging MPB from these trees were carrying predominantly *G. clavigera*. For example, more than 38% of MPB attacking trees in 2010 were carrying *O. montium*, yet only 4.3% of adults emerging from these same trees were observed with *O. montium* in their mycangia. A similar pattern was seen in trees attacked in 2011 (Table 2).

Table 5
Comparison of model R^2; best values appear in bold. Number of MPB emerging carrying *G. clavigera*, *O. montium*, and no fungus were compared to feedign model predictions (arranged from packing early, model 1, to packing late, model 5). Values of R^2 for *G. clavigera* are high across models but lower for *O. montium* and poor for 'no fungi'. This difference can be attributed to the high number of *G. clavigera* emergence observations for 2010 relative to *O. montium*.

Dataset	**Comparison of R^2 (2010 data)**				
	Model 1	Model 2	Model 3	Model 4	Model 5
R^2_{GC}	**0.9973**	**0.9973**	**0.9973**	0.9791	**0.9972**
R^2_{OM}	0.6600	0.6573	0.6603	0.6086	**0.6624**
R^2_{none}	0.0758	0.0711	0.1399	**0.1521**	**0.1521**

3.2. Model performance

Using parameterized data, model fit statistics including ΔAIC (Table 4) and R^2 (Table 5) were computed. We found that all five models performed well, in terms of visual fit (Fig. 5) and high R^2 (Table 5), when predictions were compared to field observations used for model parameterization. Model 5, representing the case where MPB pack their mycangia with the last fungus contacted, performed best in terms of producing the lowest AIC (Table 4) and model 4 also performed quite well. Differences in R^2 were trivial (Table 5).

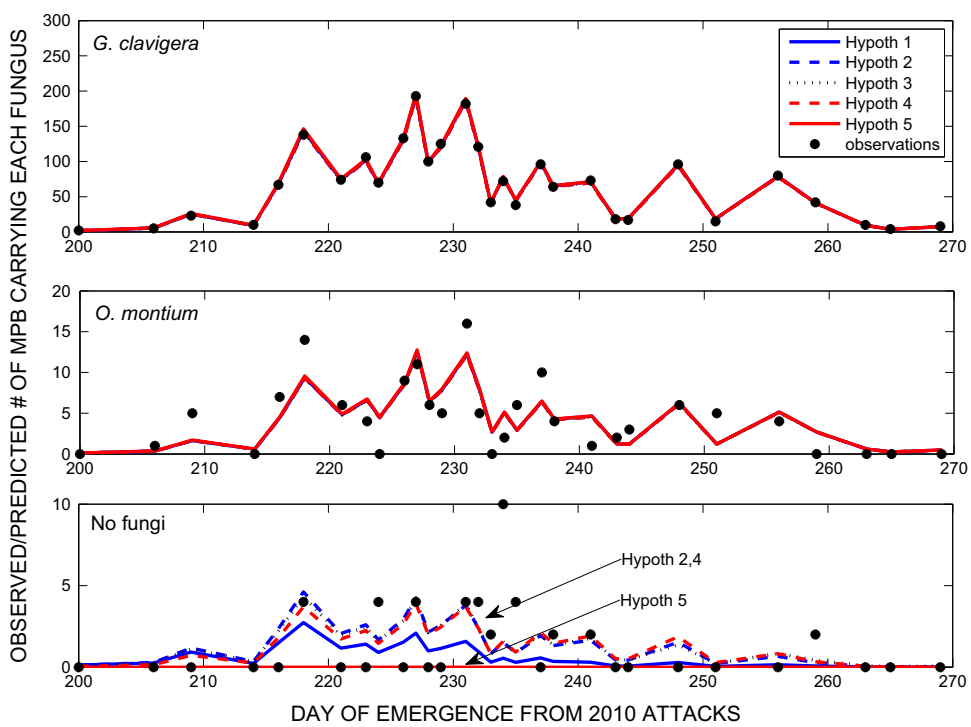

Fig. 5. Comparison of the five model predictions for fungi carried by emerging beetles versus actual observations using the parameterization dataset (2010). Models are arranged in order of mycangial packing with model 1 representing immediate packing and model 5 presenting packing just prior to emergence from the tree. Here we see all models perform very well for predicting *G. clavigera* with emerging beetles, as well as for beetles emerging with *O. montium* but have more difficulty predicting when beetles emerge with no fungus (in part because model predictions for 'no fungus' are directly affected by predictions for *G. clavigera* and *O. montium*).

Table 6
Parameter confidence intervals (95%) from bootstrapped 2010 data. Models are arranged from 1 ("first fungus contacted") to 5 ("last fungus contacted"). Across models, the ratios β_{GC}/β_{OM} are larger, suggesting that *G. clavigera* grew much more quickly under the bark than *O. montium*, even though their growth on agar was comparable.

Dataset	**Parameter confidence intervals**				
	Model 1	Model 2	Model 3	Model 4	Model 5
β_{GC}	(0.9167,0.9377)	(1,1)	(0.9981,1.000)	(0.7209,0.8853)	(0.5896,0.6377)
β_{GC}	(0.0354,0.0477)	(0.0369,0.0512)	(0.0373,0.0515)	(0.0323,0.0391)	(0.0240,0.0328)
$\frac{\beta_{GC}}{\beta_{OM}}$	(17.22,28.98)	(17.57,31.27)	(16.38,30.43)	(17.44,29.52)	(17.66,29.96)
λ	na	(3.6053,4.5847)	(.5777,1.5862)	(4.0081,4.9052)	na
μ	na	na	(3.1076,7.9357)	na	na

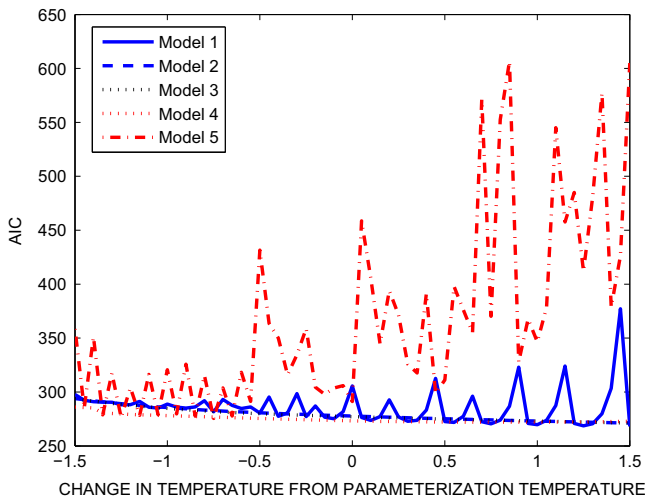

Fig. 6. Variability in AIC when models 1–5 were run with temperature data used in model parameterization with a small +/− change in temperature. Note the high degree of sensitivity of model 5 ("last fungus contacted") and, to a lesser degree, model 1 ("first fungus contacted"). Models 2 ("mostly first fungus contacted"), 3 ("some delay in mycangial packing"), and 4 ("mostly last fungus contacted") were much less sensitive with model 4 being the most robust to small fluctuations in temperature.

3.3. Model validation

After bootstrapping and reparameterizing the models 1000 times using data from trees attacked in 2010 (i.e., the data used in the original parameterization), the 95% confidence intervals were compared (Table 6). These intervals showed small amounts of variability across parameter estimates for models 1, 2, 3 and 5 and greater variability in model 4. This was expected for model 4 due to the range of viable parameter estimates obtained from the original dataset, perhaps indicating a very shallow likelihood surface.

When each model was run for a range of temperature shifts from −1.5 to 1.5 °C, we found that the AIC values for each model fluctuated in different ways. Models 1 and 5 were the most variable, and model 4 was the least variable (Fig. 6). Over the entire temperature range, the AIC values for model 4 varied by 3.83, models 2 and 3 varied by 23.69 and 24.16, respectively. Models 1 and 5 were the most sensitive with an overall change in AIC of 67.59 and 284.31. The sensitivity in model 5 was quite pronounced, even with a small change in temperature of −0.1–0.1 °C. The change in AIC over this range was 205.20. The models were further evaluated using an independent dataset based on observed MPB attack and emergence and fungi data, and hourly temperatures for trees attacked in 2011. ΔAIC (Table 7) and R^2 values (Table 8) were computed. These provided somewhat conflicting results with model 4 ("mostly last fungus contacted") providing the best AIC value by a sizeable margin and model 5 ("last fungus contacted") providing the best R^2 values. Model predictions were less accurate than when visually compared to the observed data used in model parameterization (Fig. 5). All five models overpredicted *G. clavigera* with emerging beetles and underpredicted emergence with *O. montium* and no fungi (Fig. 7). This is not represented in the R^2 values for the models, however, because R^2 is a measure of whether the timing of increases and decreases is accounted for, not the scale.

4. Discussion

4.1. Mycangial packing hypotheses and model fit

All five models describing various mycangial packing strategies provided good predictions of emerging MPB carrying *G. clavigera*, and reasonable predictions for MPB carrying *O. montium*. The model that assumed MPB packed their mycangia with the last fungus encountered (model 5) had the lowest AIC and two of the best R^2 values. None of the models did a good job of predicting MPB emergence with 'no fungi', likely because few beetles emerging from trees attacked in 2010 (i.e., data used for model parameterization) had no fungi. The overwhelming majority of MPB emerging from 2010 attacks were found to be carrying *G. clavigera* which put more weight on matching *G. clavigera* emergence in parameter estimation. In addition, our model defined the proportion of 'no fungi' in the tree as the proportion of the tree not already colonized by the two fungi, making 'no fungi' predictions very reliant on predictions for the two fungi.

The two models assuming either the first or last fungus encountered were packed in the mycangia were the most sensitive to temperature changes. Altering the hourly temperatures could effectively alter the prevalence of a particular fungal species at the time of emergence, particularly if the tree was still being colonized by the fungi near the time of MPB emergence from the tree, as was the case for model 5. Altering the temperature series by warming or cooling had the potential to change the timing of tree colonization, thereby dramatically changing model predictions of the fungal species being carried out of the tree which could change the fit of the model (Fig. 6). Spreading mycangial packing over time (i.e., models 2–4) buffered fluctuations in fungal prevalence to small changes in temperature. In addition, fungal growth rate scaling parameters for these models were larger, which led to higher tree colonization by fungi during the teneral adult feeding window (literally leaving less room for fluctuations in fungal prevalence and hence, model fit; Fig. 6). We also see in this figure how 'no fungi' predictions are tied to predictions of *G. clavigera* and *O. montium*. Models 1 and 5 have the shared property that all MPB pack their mycangia (either when they first enclose from pupa chamber or just prior to emergence from the tree), so predictions of no fungi must can only arise if the tree was not fully colonized by fungi. The models with mycangial packing spread over time (models 2–4), however, allow some portion of MPB to never pack their mycangia depending on duration of the teneral adult feeding window – despite the tree being fully colonized by fungi. This explains how models 2–4 are able to predict higher numbers of beetles emerging with no fungi than models 1 and 5.

Repeating the model comparisons for trees attacked in 2011, we found a much starker contrast between models in terms of AIC

Table 7
Comparison of $\Delta AIC = AIC - AIC_{low}$ computed for the various mycangial packing models (arranged from packing early, model 1, to packing late, model 5) for 2011 validation data with the best value marked in bold. For the validation data, model 4 produced the lowest AIC, $AIC_{low} = 1383.2$.

Comparison of ΔAIC (**for validation data**)				
Model 1	Model 2	Model 3	Model 4	Model 5
1170.1	122.9	155.5	**0**	838.3

Table 8
Comparison of R^2 fit for each model (arranged from packing early, model 1, to packing late, model 5) against the validation data where the best values are marked in bold.

Dataset	**Comparison of** R^2 (**for validation data**)				
	Model 1	Model 2	Model 3	Model 4	Model 5
R^2_{GC}	0.9635	0.9637	0.9636	**0.9642**	**0.9642**
R^2_{OM}	0.9261	0.9258	0.9256	0.9257	**0.9262**
R^2_{none}	0.1962	0.6617	0.6397	**0.7079**	**0.7174**

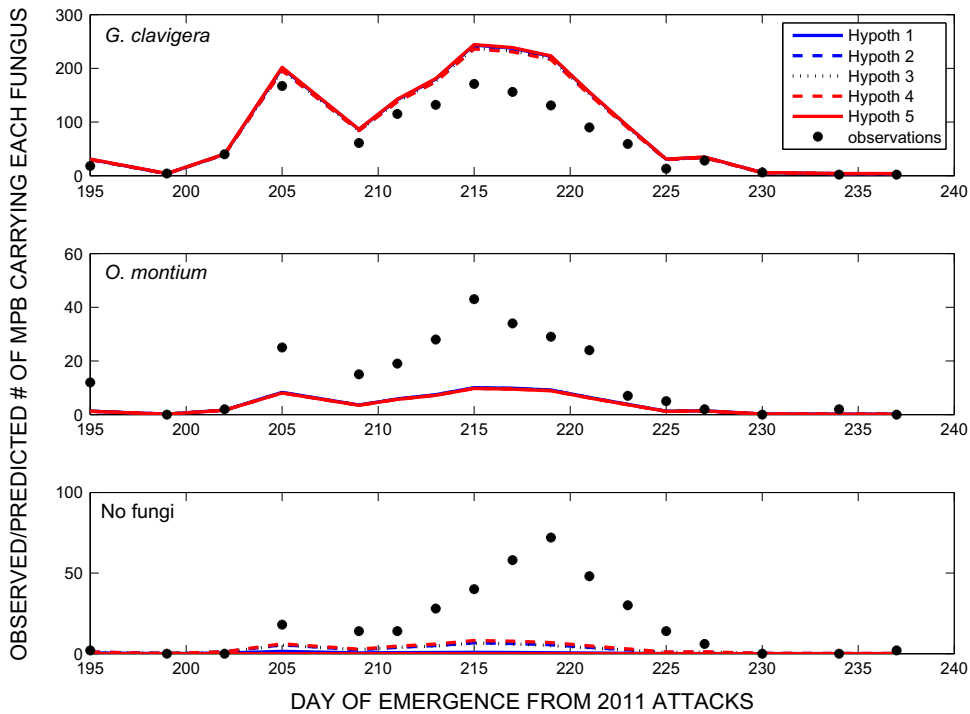

Fig. 7. Comparison of the five model predictions for fungal emergence versus observed emergence using the validation dataset from trees attacked in 2011. Models are arranged in order of mycangial packing with model 1 representing immediate packing and model 5 presenting packing just prior to emergence from the tree. We note that temperatures in 2011–2012 were warmer than in 2010–2011 which resulted in slightly higher relative emergence by *O. montium*. This resulted in an overprediction in the number of MPB emerging with *G. clavigera* and an underprediction of the number of beetles emerging with *O. montium* and no fungi. The differences in model predictions are most noticeable in plot C) where the predicted emergence of MPB carrying no fungi is shown. Note that models 1 and 5 ("first fungus contacted" and "last fungus contacted") predict that nearly zero beetles will emerge with no fungi (likely due to full tree colonization).

(Table 7). Model 4, where observed fungus comes from more recent feeding, produced the lowest AIC by a substantial margin (119.5 lower than the next model, model 2). Model 5, which performed best in terms of AIC when the data used in parameterization was also used for validation, had the highest R^2 but the lowest AIC of all five models (Table 8). Correlation coefficient may not be the best statistic for model selection, however, since it responds to timing of increases and decreases in fungal prevalence rather than actual magnitudes. A visual inspection of predictions versus observations (Fig. 7) shows that all models overpredict prevalence of *G. clavigera* and underpredict *O. montium* emergence, although the shapes of the distributions are qualitatively correct. Model 4 overpredicted *G. clavigera* and underpredicted 'no fungi' by the smallest margin of the five models, thereby producing the lowest AIC.

Based on the two validation exercises, models 4 and 5 seemed to provide the best fit. In addition, β_{GC} estimates for models 1, 2 and 3 were all unrealistically large (i.e. very close to one). These results suggest that the most likely fungus for dispersal is the fungus available just prior to emergence and that the most likely value for β_{GC} ranges from approximately 0.6 to 0.8. Model 5 was highly sensitive to slight changes in temperature (Fig. 6), however, lowering its reliability. Therefore, the best choice is model 4 which assumes that adult MPB acquire mostly the last fungus it encounters, although with an exponential decay in acquisition.

At our field site, the number of MPB emerging from study trees and carrying *O. montium* was lower than the number carrying *G. clavigera*. This finding was unexpected, especially given that most of the attacking beetles both years were carrying predominantly *O. montium*. A possible explanation includes factors related to the location of the study area. The study trees were located in a cool drainage, and therefore potentially favored growth of the cool-loving *G. clavigera* once beetles were in the tree. MPB-attacked trees on a nearby south-facing slope may have provided many of the beetles that attacked trees used in our study and may have provided a more conducive growing environment for the warm-loving *O. montium*. Cooler temperatures in the study trees, however, favored growth of *G. clavigera*, causing it to dominate the emergence data.

Differences in the β estimates between the fungal species could also be attributed to the lack of beetles observed carrying *O. montium* as they emerged from trees. Since the growth rate scaling parameters were estimated by determining parameter values which best fit the model to the data, low numbers of beetles emerging with *O. montium* necessarily led to low estimates for the *O. montium* growth rate scaling parameter, β_{OM}.

In Addison et al. (2013), we hypothesized that variability in temperature could allow both *G. clavigera* and *O. montium* to remain present in the MPB-fungus mutualism while also exploring the effect of various spacings between fungal individuals inoculations (i.e., densities of attacking MPB). In that analysis we found that both fungi could remain if MPB periodically transitioned between warm and cold environments. Growth rates of the two fungi, scaled using β estimates from the current study (Table 3), provide an additional explanation. Although lab data suggests that *O. montium* can grow faster than *G. clavigera* at temperatures above 15 °C, when growth is scaled by β, *G. clavigera* grows significantly faster until 30 °C (Fig. 8). The faster growth of *G. clavigera*, even at warm temperatures, would allow *G. clavigera* to persist in the mutualism under a wide range of conditions. It is unclear if these same differences in growth scaled to a tree would persist at a different field location.

Unscaled (Plot A) and scaled fungal growth rates (Plot B) using model 5 estimates ($\beta_{GC} = 0.6355$ and $\beta_{OM} = 0.0263$) appear in Fig. 8. Plot B would look similar for all model estimates because the ratio of growth rate scaling parameters was approximately 25:1 for all models. These plots show how *G. clavigera* persists in

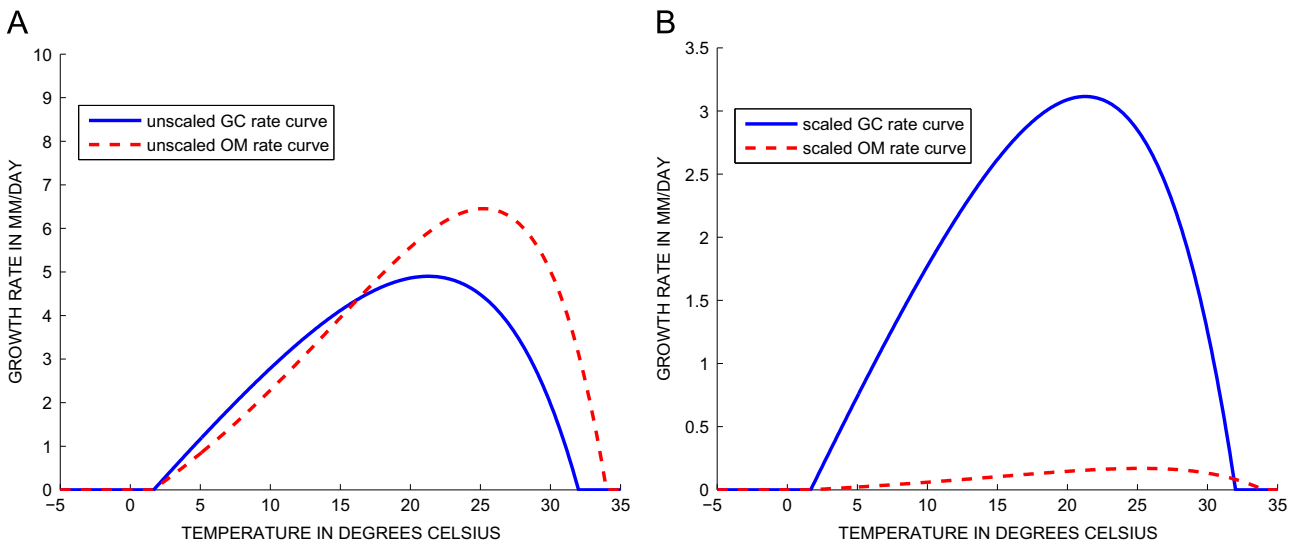

Fig. 8. Unscaled (i.e., rates observed in culture; Plot A) and scaled (Plot B) rates of growth for the two fungi using estimates from model 5 (based on validation data) where $r_{GC}(T) = \beta_{GC} \cdot r_{GC,culture}(T) = 0.6355 \cdot r_{GC,culture}(T)$, and $r_{OM}(T) = \beta_{OM} \cdot r_{OM,culture}(T) = 0.0263 \cdot r_{OM,culture}(T)$. Although the growth rates on agar are comparable, realized growth rates in the field give *G. clavigera* a substantial advantage.

the mutualism despite warming conditions; its advantage under the bark allows it to grow faster than *O. montium* until the temperature reaches approximately 32 °C, when it becomes too warm for *G. clavigera* to grow. These results underscore the need to have accurate parameter estimates, specifically those that define the coldest and warmest temperatures where the two fungi can grow (T_0 and T_m from Eq. (1), as these most prominently distinguish the two fungi when their growth is scaled.

5. Conclusions

We tested several hypotheses regarding the timing of mycangial packing with fungal spores and estimated parameters to connect fungal growth rates in trees with growth rates measured in lab culture. Each hypothesis was tested by developing a mathematical representation and parameterizing the corresponding model using field observations of fungal species being carried by MPB attacking and emerging from trees. Model predictions were evaluated via correlation coefficients, ΔAIC, sensitivity analysis and validation using an independent field observations from the same site but a different year. While all models adequately predicted proportion of fungi carried from a tree when evaluated using calibration data, the two mycangial packing hypotheses which corresponded to later mycangial packing (model 4, mostly last fungi contacted, and model 5, last fungi contacted) were most plausible. Estimated growth rate scaling parameters for the models suggest that at the location used in this study *G. clavigera* was as much as twenty-five times faster growing than *O. montium*. However, production of *O. montium* was anomalously low and could have biased this result.

We developed a method, based on observed data, for combining models to describe two overlapping phenologies and incorporating a nontrivial interaction between them. In the specific case of MPB this allowed us to deduce cryptic growth rates of fungi under the bark and to hypothesize that the fungi last fed upon are most likely to be dispersed (and therefore have the highest fitness). In neither case would it have been possible to determine these results using direct observation, and both are contrary to what might have been expected from laboratory study. In general this type of approach can be used for systems with temperature dependent transmission of diseases and parasites, fertilization of plants by specialist pollinators, and efficacy of biocontrol agents against pests, to name but a few. In all these examples, outcomes are controlled by overlapping phenologies and unknown probabilities of interaction during a thermally mediated window of opportunity. Our modeling approach provides a tractable pathway for developing and testing hypothesis of such critical ecological interactions.

Acknowledgments

We would like to thank Jim Vandygriff, Matt Hansen, Joel Martin and Greta Schen-Langenheim for field support and mycangial dissections. We would also like to thank Melissa Moore for fungal identification. Funding was provided by the USDA Forest Service, Western Wildland Threat Assessment Center and a National Science Foundation Grant, DEB 0918756.

References

Adams, A.S., Six, D.L., 2007. Temporal variation in mycophagy and prevalence of fungi associated with developmental stages of *Dendroctonus ponderosae* (coleoptera curculionidae). Environ. Entomol. 36 (1), 64–72.
Adams, A.S., Six, D.L., Adams, S.M., Holben, W.E., 2008. In vitro interactions between yeasts and bacteria and the fungal symbionts of the mountain pine beetle (*dendroctonus ponderosae*). Microb. Ecol. 56 (3), 460–466.
Addison, A., Powell, J., Six, D., Moore, M., Bentz, B., 2013. The role of temperature variability in stabilizing the mountain pine beetle-fungus mutualism. J. Theor. Biol. 335, 40–50.
Bentz, B., Vandygriff, J., Jensen, C., Coleman, T., Maloney, P., Smith, S., Grady, A., Schen-Langenheim, G., 2013. Mountain pine beetle voltinism and life history characteristics across latitudinal and elevational gradients in the western united states. Forensic Sci. 60 (2).
Bentz, B.J., Logan, J.A., Amman, G.D., 1991. Temperature-dependent development of the mountain pine beetle (coleoptera: Scolytidae) and simulation of its phenology. Can. Entomol. 123 (05), 1083–1094.
Bleiker, K., Six, D., 2009. Competition and coexistence in a multi-partner mutualism: interactions between two fungal symbionts of the mountain pine beetle in beetle-attacked trees. Microb. Ecol. 57 (1), 191–202.
Bleiker, K.P., Six, D.L., 2007. Dietary benefits of fungal associates to an eruptive herbivore: potential implications of multiple associates on host population dynamics. Environ. Entomol. 36 (6), 1384–1396.
Burnham, K.P., Anderson, D.R., 2002. Model Selection and Multimodel Inference: A Practical Information-Theoretic Approach. Springer, New York.
Calabrese, J.M., Fagan, W.F., 2004. Lost in time, lonely, and single: reproductive asynchrony and the allee effect. Am. Nat. 164 (1), 25–37.
Cook, S.P., Shirley, B., Zambino, P., 2010. Nitrogen concentration in mountain pine beetle larvae reflects nitrogen status of the tree host and two fungal associates. Environ. Entomol. 39, 821–826.

Cudmore, T.J., Björklund, N., Carroll, A.L., Staffan Lindgren, B., 2010. Climate change and range expansion of an aggressive bark beetle: evidence of higher beetle reproduction in naïve host tree populations. J. Appl. Ecol. 47 (5), 1036–1043.
de la Giroday, H.-M.C., Carroll, A.L., Aukema, B.H., 2012. Breach of the northern rocky mountain geoclimatic barrier: initiation of range expansion by the mountain pine beetle. J. Biogeogr. 39 (6), 1112–1123.
Gross, R.S., Werner, P.A., 1983. Relationships among flowering phenology, insect visitors, and seed-set of individuals: experimental studies on four co-occurring species of goldenrod (solidago: Compositae). Ecol. Monogr., 95–117.
Kaspari, M., Pickering, J., Longino, J.T., Windsor, D., 2001. The phenology of a neotropical ant assemblage: evidence for continuous and overlapping reproduction. Behav. Ecol. Sociobiol. 50 (4), 382–390.
Köhl, J., Lombaers-Van Der Plas, C., Molhoek, W., Kessel, G., Goossen-Van Der Geijn, H., 1999. Competitive ability of the antagonists ulocladium atrum and gliocladium roseum at temperatures favourable for botrytis spp. development. BioControl 44 (3), 329–346.
Krokene, P., Solheim, H., 1998. Pathogenicity of four blue-stain fungi associated with aggressive and nonaggressive bark beetles. Phytopathology 88 (1), 39–44.
Lehning, A., Zimmer, W., Zimmer, I., Schnitzler, J.-P., 2001. Modeling of annual variations of oak (quercus robur l.) isoprene synthase activity to predict isoprene emission rates. J. Geophys. Res.: Atmos. (1984–2012) 106 (D3), 3157–3166.
Logan, J., Wollkind, D., Hoyt, S., Tanigoshi, L., 1976. An analytic model for description of temperature dependent rate phenomena in arthropods. Environ. Entomol. 5 (6), 1133–1140.
Logan, J.A., Bentz, B.J., 1999. Model analysis of mountain pine beetle (coleoptera: Scolytidae) seasonality. Environ. Entomol. 28 (6), 924–934.
Meddens, A.J., Hicke, J.A., Ferguson, C.A., 2012. Spatiotemporal patterns of observed bark beetle-caused tree mortality in British Columbia and the western united states. Ecol. Appl. 22 (7), 1876–1891.
Molnár, P.K., Kutz, S.J., Hoar, B.M., Dobson, A.P., 2013. Metabolic approaches to understanding climate change impacts on seasonal host-macroparasite dynamics. Ecol. Lett. 16 (1), 9–21.
Moore, M.L., 2013. The Effects of Temperature on Fungal Symbionts in the Mountain Pine Beetle-Fungus Multi-partite Symbiosis (Ph.D. thesis). The University of Montana.
Murali, K., Sukumar, R., 1994. Reproductive phenology of a tropical dry forest in mudumalai, southern india. J. Ecol., 759–767.
Raffa, K.F., Berryman, A.A., 1983. The role of host plant resistance in the colonization behavior and ecology of bark beetles (coleoptera: scolytidae). Ecol. Monogr. 53 (1), 27–49.
Régnière, J., Powell, J., Bentz, B., Nealis, V., 2012. Effects of temperature on development, survival and reproduction of insects: experimental design, data analysis and modeling. J. Insect Physiol. 58 (5), 634–647.
Rice, A., Thormann, M., Langor, D., 2008. Mountain pine beetle-associated blue-stain fungi are differentially adapted to boreal temperatures. For. Pathol. 38, 113–123.
Salinger, D.H., Anderson, J.J., 2006. Effects of water temperature and flow on adult salmon migration swim speed and delay. Trans. Am. Fish. Soc. 135 (1), 188–199.
Sambaraju, K.R., Carroll, A.L., Zhu, J., Stahl, K., Moore, R.D., Aukema, B.H., 2012. Climate change could alter the distribution of mountain pine beetle outbreaks in western canada. Ecography 35 (3), 211–223.
Six, D., 2012. Ecological and evolutionary determinants of bark beetle-fungus symbioses. Insects 3 (339–366).
Six, D., Paine, T., 1998. Effects of mycangial fungi and host tree species on progeny survival and emergence of *dendroctonus ponderosae* (coleoptera: Scolytidae). Environ. Entomol. 27 (6), 1393–1401.